Intelligence System towards Identify Weeds in Crops and Vegetables Plantation Using Image Processing and Deep Learning Techniques

K. Veerasamy[1*] and E.J. Thomson Fredrik[2]

[1*] Ph. D Research Scholar, Department of Computer Science, Karpagam Academy of Higher Education, Coimbatore, India. ksveerasamy27@gmail.com,
Orcid: https://orcid.org/0000-0001-8798-5970

[2] Professor, Department of Computer Applications, Karpagam Academy of Higher Education, Coimbatore, India. thomson.ej@kahedu.edu.in, Orcid: https://orcid.org/0000-0003-1309-1936

Received: July 22, 2023; Accepted: September 29, 2023; Published: December 30, 2023

Abstract

Due to uneven spacing of the plants, identification of weeds and bushes in crops and vegetables plantations is more difficult than identification of weeds and bushes in crops. There has not been much research done on weed identification in vegetable plantations thus far. Although there is a wide variety of plant species, the traditional crop weed detection techniques are used to directly identify weeds. This research introduces a novel approach that combines image processing and deep learning techniques. Instead of directly tackling weed detection, the proposed method focuses on identifying vegetables. The process begins by utilizing a trained CenterNet model to detect and create bounding boxes around the vegetables. Subsequently, any remaining green objects outside the bounding boxes are classified as weeds. By narrowing the scope to vegetable detection, the model avoids the complexities associated with different weed species. Moreover, this approach offers the advantage of reducing the complexity of weed detection and minimizing the required training image dataset, leading to improved performance and accuracy in weed identification. To separate the weeds from the background, a color index-based segmentation technique is employed using image processing methods. Using Genetic Algorithms (GAs), the employed colour index is chosen and assessed in accordance with the Bayesian classification error. The trained CenterNet model gets score 0.953 in Figure 1, a recall of 95.2%, and a precision of 95.8% during field test. In comparison to the widely used ExG index, the PI (Proposed Index) is 19R + 24G + 2B = 864 produces outstanding segmentation accuracy at significantly less cost for computation segmentation. Outcomes of this experiment show that the suggested strategy for weed identification in vegetable plantations may be used successfully on the ground.

Keywords: CenterNet, Segmentation, Classification, Weed Identification, Chromosome, Crops, Plantations, Crossover, Mutation.

1 Introduction

Vegetables are highly regarded as one of the most nutrient-dense foods worldwide, primarily due to their rich content of vitamins, minerals, and antioxidants. As living standards improve, the consumption of

Journal of Wireless Mobile Networks, Ubiquitous Computing, and Dependable Applications (JoWUA), volume: 14, number: 4 (December), pp. 45-59. DOI: *10.58346/JOWUA.2023.I4.004*

*Corresponding author: Ph. D Research Scholar, Department of Computer Science, Karpagam Academy of Higher Education, Coimbatore, India.

green vegetables becomes increasingly prevalent in diets. This highlights their significance in daily life and underscores their economic value. Crops and vegetable plants are susceptible to pest and disease infestation because plants compete with weeds for nutrients, sunshine, and water (Berge, T.W., 2008) (Hamuda, E., 2016). In the event of competition between vegetable - weeds, the vegetables output reduced by 45% to 95% (Dai, X., 2019). The excessive use of chemical herbicides can result in overapplication in areas with minimal weed infestation. This practice has detrimental effects on the ecosystem, including soil and groundwater contamination (Dai, X., 2020). Additionally, organic food production requires weed management without the use of chemicals. Consequently, hand weeding continues to be the predominant method for weed management in vegetable plantations, despite the higher labor costs involved (Dai, X., 2020). Developing a visual approach to differentiate between weeds and vegetables is a crucial step towards ecologically sustainable weed management.

Extensive research has been conducted on machine vision algorithms for weed detection (Hamuda, E., 2016) (Dai, X., 2019) (Yu, S.H., 2021) and (Serpen, G., 2018). Ahmed et al. (Veeranampalayam Sivakumar, A.N., 2020) achieved a 97.3% accuracy in identifying six weed species using a Support Vector Machine (SVM) on a database of 224 images with the optimal set of extractors. Herrera et al. (Olsen, A., 2019) built a weed-crop classifier employing fuzzy decision-making and shape descriptors, achieving a classification accuracy of 92.9% on a collection of 66 photos. Chen et al. (Lammie, C., 2019) developed a weed and crop discrimination approach utilizing a binocular stereo vision system based on height characteristics. By analyzing the depth dimension and employing a height-based segmentation technique, they successfully distinguished between weeds and crops. Taking advantage of plant spacing information, the relative height of weeds was used to separate them from the crops.

Deep learning has demonstrated remarkable capabilities in automatically extracting complex features from images (Rączkowski, Ł., 2019) (Bermant, P.C., 2019) (Sahlsten, J., 2019). It is widely regarded as a promising technique for object recognition and image categorization. Deep learning techniques for image detection can be categorized into two groups (Yu, S.H., 2021). The first group involves object classification, followed by drawing bounding boxes around objects for classification. The second group is semantic segmentation, which focuses on classifying object pixels (Pawłowski, J., 2022). Olsen et al. (Gu, H., 2022) achieved an average classification accuracy of 96.2% and 96.6% using benchmark deep learning models to classify photos of sixteen different weed varieties. Ferreira Santos et al. (Yu, X., 2020) used Convolutional Neural Networks (CNNs) to identify weeds among potato plant photographs, classifying them as grass or broadleaf. Asad and Bais (Nampei, M., 2019) compared the performance of deep learning meta-architectures such as UNET and SegNet with encoder blocks like ResNet-50 and VGG16 using high-resolution color photos of potato fields. Khurana and Bawa (Liakos, K.G., 2018) employed morphological scanning and textural feature analysis of sugar beet plants, using KNN classification to distinguish weeds in field crops. V. Sivakumar (Benos, L., 2021) examined and compared two object detection algorithms, namely Faster SSD – Single Shot Detector and RCNN, for detecting weeds in soybean fields using UAV data. Inference speed and mean IoU (Intersection over Union) were used to evaluate the models' performance. Osorio et al. (Gutiérrez, S., 2021) presented three approaches for weed estimation in lettuce fields using image processing and deep learning (Bae, D., 2021). The first approach relied on the SVM algorithm, the second used YOLOv3, and the third employed Mask R-CNN. These approaches improved the accuracy of weed estimation and reduced subjectivity compared to estimates from human experts.

In the growing of vegetables, there is no standard for clear plant spacing and row spacing. Identification of weeds in crops and vegetables plantations is very difficult than in crop plantations because vegetables and weeds grow irregularly. Additionally, during robotic harvesting, vegetable

plantations and weeds will also be mixed in with crops of vegetable plantations and should be removed manually. Sales prices have increased as a result of various labour expenditures. Although a lot of variation among variety of weeds, research on weed identification in vegetable plantations is still in its infancy. Previous crop weed identification methods tended to concentrate mostly on weed identification directly. The remaining plants segmented images in the agriculture fields are indentified as weeds. As a result, we suggested methods for employing deep learning algorithm, which is Convolutional Neural Networks architecture, to first detect and segment the vegetable. This method can greatly minimize the amount of the training image dataset and the difficulty of weed detection, improving the effectiveness and accuracy of weed identification.

The creation of automatic weed identification equipment is the main objective of this research study, and to remove weeds in crops and vegetables plantations using an algorithm based on image processing and deep learning. The precise goals were to use deep learning to develop a model that could recognize vegetable box boundaries and to use image processing and the color feature for removing and segmenting weeds that are outside the bounding boxes.

2 Proposed Work

Weed Identification

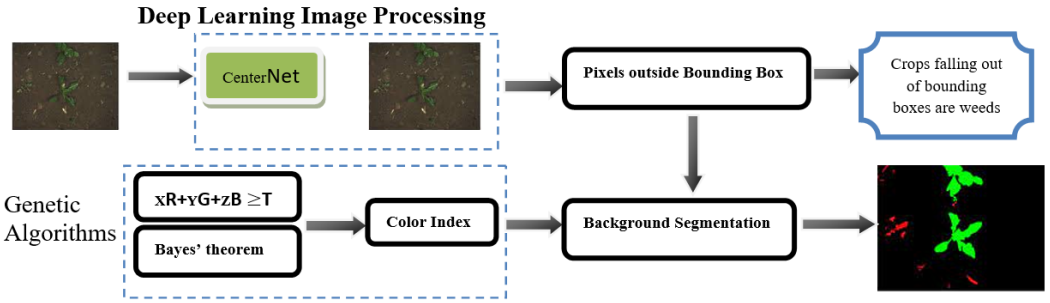

Figure 1: Architecture for Proposed Weed Detection Methodology

The method for weed identification suggested in this study consists of two stages. For the purpose of this study, bok choy is detected in the first stage using the cutting-edge, CenterNet algorithm. Architecture for object detection without anchors is CenterNet. This structure has the significant advantage of substituting a far more elegant algorithm that is inherent to the CNN flow for the traditional Suppression of Non-Maximum (SNM) at the post-processing stage. This system makes inference significantly quicker. Vegetables crops images were gathered, used as training samples in neural networks. The trained neural network is utilized to identify bok choy by generating bounding boxes around them and assigning class probabilities and bounding box locations. In the second stage, the presence of weeds in the image is visually classified by segmenting the vegetation pixels outside the boundary boxes. This segmentation process is based on color information, and a color index is applied to distinguish weeds from other vegetation. Using Genetic Algorithms (GAs), the employed colour index is chose and assessed in accordance with the Bayesian Classification Error. Using a graphics processing unit, the CenterNet model is trained and tested in the phytoruch deep learning environment, as detailed in the proposed method's procedural steps (USA, NVIDIA; Santa Clara, NVIDIA GeForce RTX 2080 SUPER). Python and the OpenCV library were used to create and implement a genetic algorithm. Both methods were run on a machine equipped with high configuration system like Intel@Core TM i9 Processor speed,3.60 GHZ_CPU.

Image Acquisition

A digital camera was used to capture pictures of bok choy, often known as Indian cabbage white (Brassica rapa spp. chinensis). The vegetable plantation, where the photos were taken is situated in Kodaikanal, India, at latitude 10.2381° N, and longitude 77.4892° E. The photos' original sizes were 3024 x 4032 pixels. Images of bok choy were captured in a variety of settings, including diverse lighting conditions (Fig. 2: a1, a2), complicated backdrops (Fig.2: a3), and different growth phases, Fig.2: a4.

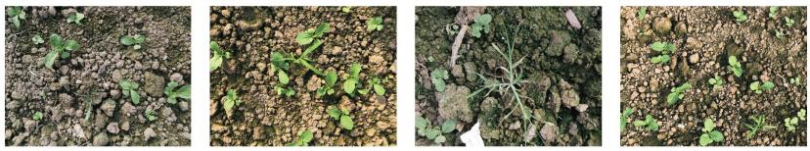

(a1) (a2) (a3) (a4)

Figure 2: Vegetable Crops Images from Various Lighting Conditions

Fig.2: a1-Less brightness, Fig.2: a2-full brightness, Fig.2: a3-difficult locations and Fig.2: a4-different size of growing stages

Deep Learning in Crops and vegetables Detection

- **Image Amplification**

To make the experimental dataset more richly diverse, the 1150 photos from the training dataset were increased to 11500 images by utilizing data augmentation techniques. Following pre-processing of the gathered photos for rotation, image definition, colour, rotation, and brightness, the dataset was expanded as depicted in figure 3.

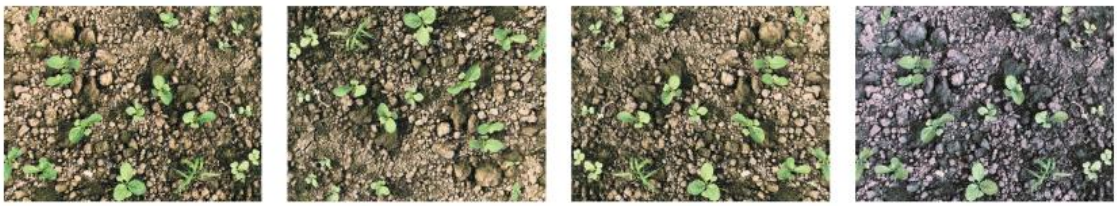

(Fig.3: a1) (Fig.3: a2) (Fig.3: a3) (Fig.3: a4)

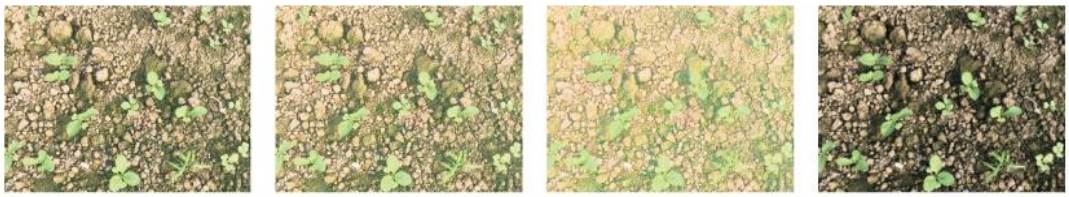

(Fig.3: a5) (Fig.3: a6) (Fig.3: a7) (Fig.3: a8)

Figure 3: Augmentation Techniques of Images (Exact image to blur image)

- **Annotation of Image**

Using unique piece of software called Label Image, bounding boxes were manually annotated against the crops in the enter photos. To train the CenterNet, related XML format label files were created. The training data and testing data phases each required 80% and 20% of the dataset, respectively.

- **Preparation for Training and Testing**

The CenterNet model is a state-of-the-art object detector that relies on key point estimates and is anchor-free. In CenterNet, each object is represented by a single point, and object centres are predicted using a heatmap. Estimated centers are computed from the heatmap's peak values using a Gaussian filter to the extended kernel neighborhood and a Filter Convolution Neural Network. Using the centre localization, it is possible to directly regress object characteristics like size and dimension (Gutiérrez, S., 2021).

A single-stage detection model is CenterNet that offers substantially faster detection because Suppresion of Non-Maximum (SNM) is not necessary for after-processing stage. Hourglass is chosen as the study's backbone architecture for feature extraction. Using focal loss LK and Gaussian kernel, each ground truth key point is transformed into a smaller key-point heat map in order to train the network. In order to lessen the mistake brought on by resampling the input image's size to create the key-points heatmap, CenterNet also forecasts the local offset. An Loff loss is used to train the offset lastly, the size of the thing is reduced with loss Lsize from the centre points. As a result, the loss key-point (Lk), loss offset (Loff), and loss size of objects (Lsize) make up the loss function (Ldet):

$$L_{det}=L_k+\lambda_{size}L_{size}+\lambda_{off}L_{off} \quad (1)$$

Where size and off are loss weighting constants. As recommended by the author, size=0.1 and off=1are utilized in this paper. Table 1 displays the formulae for each distinct loss and their interpretation.

Table 1: Individual Loss Definition

Loss	Equation	Parameters	Meaning
L_k	$\frac{-1}{N}\sum \begin{cases} (1-y_{xyc})^{\alpha} log(\hat{y}_{xyc}), if y_{xyc}=1 \\ (1-y_{xyc})^{\beta}(\hat{y}_{xyc})^{\alpha} log(1-\hat{y}_{x}yc), otherwise \end{cases}$	N α, β	Number of keys –points Focal loss of Hyper Parameters
L_{size}	$\frac{-1}{N}\sum_{k=1}^{N}\lvert\hat{s}_{Pk}-s_k\rvert$	s_k p_k	Size of the item K Center points for entity k
L_{off}	$\frac{-1}{N}\sum_{P}\left\lvert\hat{O}_{\tilde{P}}-\left(\frac{P}{R}-\tilde{P}\right)\right\rvert$	$\tilde{P}$ $\hat{O}$	Location of the key points Forecast local offset

Each key point's location is specified at inference time by a coordinate in the integer (xi,yi). CenterNet then creates a bounding box at location using as a measure of its detection confidence, key-point values.

$$(\hat{x}i+\delta\widehat{xi}-\frac{\widehat{w}i}{2},\hat{y}_i+\delta\hat{y}i-\frac{h_i}{2},) \quad (1)$$

$$(\hat{x}i+\delta\widehat{xi}+\frac{\widehat{w}i}{2},\hat{y}_i+\delta\hat{y}i+\frac{\hat{h}_i}{2}) \quad (2)$$

Modern bounding-box based detectors were shown to be more complicated, slower, and inaccurate than the state-of-the-art CenterNet. As the vegetable crops detector in this investigation, The CenterNet model was adopted and employed.

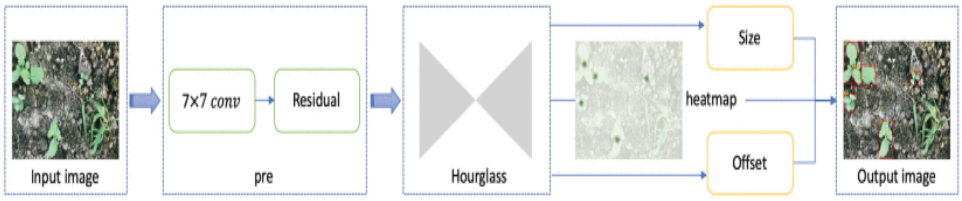

Figure 4: Shows the Center Net Identification Model

Fig. 4 depicts the CenterNet detection model. The training set's whole image library is resampled to the same fixed size. It forecasts confidence scores and bounding boxes when detecting the object. The representation of objects is a single point during the detection process, key-point estimation is then used to get the centre point of the bounding box. which is then acquired using key-point estimation. CenterNet surpasses the majority of detection techniques thanks to its usage of an anchor-free strategy that restricts its object detection to the centre point and regresses the object size.

Weed Identification Utilizing Image Processing Techniques

After identifying and labeling the vegetables, any green objects that fall outside the boundary boxes are considered weeds. To distinguish weeds from other elements in the image, such as soil, straws, stones, and other debris, a binary-coded genetic algorithm (GA) is employed. This GA operates in the RGB color space and is specifically designed for outdoor field conditions. It effectively removes weeds from the rest of the image. The segmentation result is evaluated by comparing it with the commonly used excess green (ExG) index. This comparison helps validate the accuracy of the segmentation output.

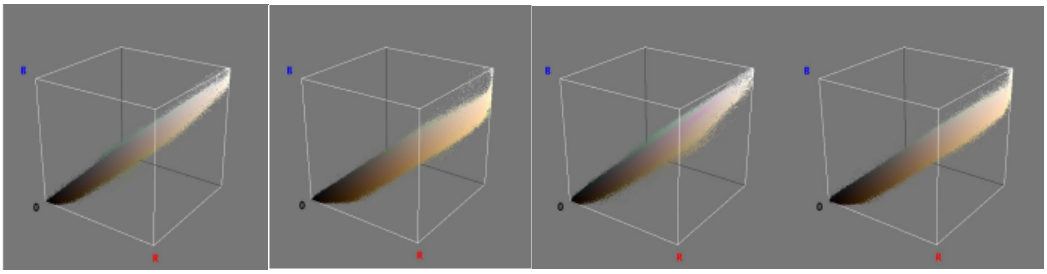

(a) (b) (c) (d)

Figure 5: Image Pixel Distribution in RGB Color Space: (a) Image Pixel Distribution of Fig. 2a, (b) Image Pixel Distribution of Fig. 2b, (c) Image Pixel Distribution of Fig. 2c, (d) Image Pixel Distribution of Fig. 2d.

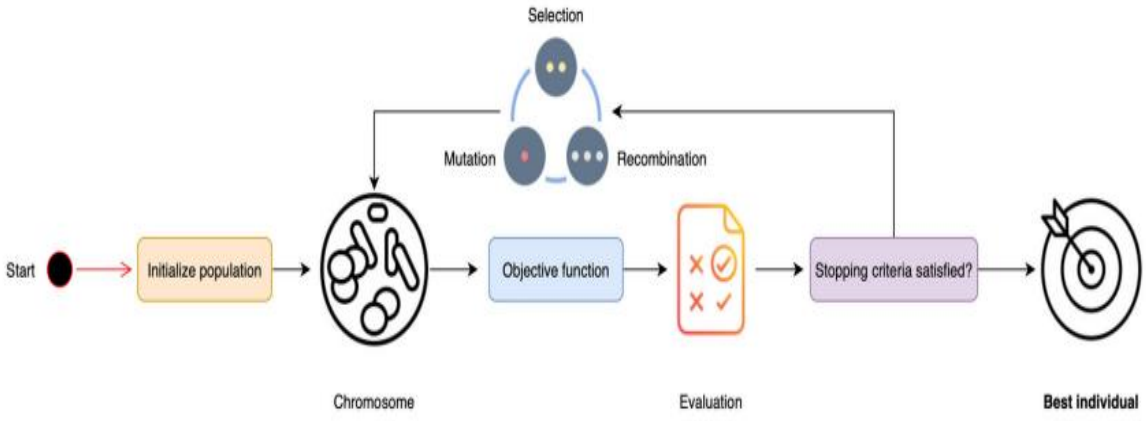

Figure 6: Procedures of a Genetic Algorithm

- **Color Index-Base Segmentation**

Distribution color space as Red Green Blue of image pixels is shown in Figure 5. Segmentation is the process of dividing an image into pixels that indicate vegetation and those that do not represent

vegetation by locating a plane that intersects the Red Green Blue colour cube. The plane is defined by the equation.

$$xR + yG + zB = T \quad (3)$$

It is necessary to identify the values of x, y, z, and T in order to distinguish plants from the surroundings.

- **Genetic Algorithms**

The family of adaptive search techniques known as Genetic Algorithms (GAs) depends on the principles of genetic evolutionary process and the natural selection. Due to their parallel search space exploration, GAs is particularly effective in solving challenging combinatorial search issues without becoming caught in local optima (Gutiérrez, S., 2021).

The three parameter ranges, x, y, and z are (255, 255), but the range of the parameter T is ([0, 1024). There will be 5105105101024 potential combinations as a result. To tackle this issue, an effective searching algorithm is required. GAs function efficiently when utilizing the acquired data in a previously unexplored domain. GA is therefore chosen to develop the search engine in this endeavour. Fig. 6 illustrates a genetic algorithms process. An initial population is produced at random to begin the procedure.

- **Chromosome**

In equation 3 parameters that were prearranged using the permutation method were represented as binary string as 88-bit, also known as a chromosome. Because GAs selects more advantageous combinations of parameters, the relative positions of the Bytes within the chromosome are essential. The first byte of the chromosome in the string is designated as the sign, where 0 denotes a negative and 1 denotes a positive, depends upon the variables range and length of the variables. The following bytes contain the parameters' binary values. The chromosomal string's structure is displayed in Table 2.

- **Population Size**

Individual is the fundamental building block of a GA, and it is distinguished by a pair of properties (parameters) known as Genes. A chromosome is created by stringing together a number of genes. The term "population" refers to a group of people. In this study, colour index parameters are generated using a population size of 200.

- **Selection**

The likelihood of a person being selected for reproduction is indirectly or directly correlated with their level of fitness in relation to the general population. In GA, the roulette wheel selection method is used to choose the person with the greatest fitness level among randomly chosen participants.

- **Crossover and Mutation**

Based on the likelihood of the crossover ratio CR, the crossover operation entails changing the parameters between the initially selected the mutant vector and target vector. The trial vector, or outcome vector, is obtained as

Table 2: Chromosome String Structure

Chromosome												
Parameter	Value 1	Value 2	Value 3	Value 4	Value 5	Value 6	Value 7	Value 8	Value 9	Value10	Value11	Value
[x]	1	1	1	1	1	0	1	1	0	0	0	-18
[y]	0	1	1	1	1	0	0	1	1	1	1	22
[z]	1	1	1	0	1	1	1	1	0	1	1	-4
[T]	1	0	0	0	1	1	0	1	1	0	0	864

In the process of crossover, the two parent bit strings are divided into separate segments of two or more bits each. Data is then exchanged between the selected chromosomes, resulting in the creation of a new population of offspring for the next generation. The offspring bit strings are generated by combining the segments of the two parent bit strings that undergo crossover. A crossover probability of 0.8 was used, indicating an 80% chance of crossover occurring between the parent chromosomes.

Mutation, on the other hand, introduces random alterations to the bit strings by inverting, shifting, or rotating one or more genetic components. This random alternation helps introduce genetic diversity within the population. In this particular application, a mutation rate of 0.2 was employed, indicating a 20% chance of mutation occurring on each bit string in the crossover operation.

- **Evaluation**

The BCEA was used to assess the function. BCEA (r, g, b) was defined for each color that was provided.

$$\text{Bayesian Classification Error Algorthm } (r,g,b) = \begin{cases} 0.5 \times P^2(r,g,b), xR + yG + zB \geq T \\ 0.5 \times P^1(r,g,b), xR + yG + zB < T \end{cases} \quad (4)$$

Where the probabilities distribution of the background, weed in the colour space corresponding, are p1 (r,g,b), and p2 (r, g, b).

$$P^1(r,g,b) = \frac{Cw}{Ct} \quad (5)$$

$$P^2(r,g,b) = \frac{Cb}{Ct} \quad (6)$$

Where the number of colour (red, green, and blue) occurrences in weed image pixels is known as Cw. The amount of colour (red, green, and blue) occurrences in background pixels is known as Cb. The sum of all the pixels in the suggested images is Ct.

The theoretical minimal rate of Bayesian Classification Error Algorithm (red, green, and blue) is obviously

$$\text{Bayesian Classification Error } (r,g,b)_{\min} = min(0.5 \text{ X} P^1(r,g,b), 0.5\text{X}P^2(r,g,b)) \quad (7)$$

In light of the reference images, the explanations of Bayesian Classification Error and its related theoretical minimum value Bayesian Classification Error$_{min}$ is as follows:

$$\text{Bayesian Classification Error} = \sum_{1=0}^{lu} \text{BCE}(ri, gi, bi) \quad (8)$$

$$\text{Bayesian Classification Error}_{\min} = \sum_{1=0}^{lu} \text{BCE}(ri, gi, bi)_{\min} \quad (9)$$

Iu stands for the quantity of distinct pixels in the reference images.

- **Criteria for Stopping**

When either of the following two requirements was met, the algorithm ends:

1. If there were reached 2000 iterations.
2. If the ideal fitness value—the theoretical lowest error of acceptance—was found, matching the predetermined threshold.

The parameters of the colour index were decoded from the best-fitting chromosomal string in Table 2 when any one of the aforementioned conditions was satisfied.

3 Results and Discussion

Crop Detection's Effectiveness

The input photos were sized down to 512512 pixels to make them suitable for the input that the Hourglass framework needs. To further analyze the training process, in terms of batch size adjusted to 4 and a maximum of 24 epochs were used. Other settings, such as momentum, learning rate at first, and weight decay regularization, etc., were CenterNet model defaults. Used the CenterNet original paper's training procedure for the model's training stage, and after the training parameters were established, the model was trained. Adam utilised an optimization technique to iteratively adjust network weights based on training data in order to minimize the training loss. Table 3 displays the initial settings for the training parameters.

The test results for the object detection task can be broken down into the following four groups: first one is (FN) False Negative, second one is (FP) False Positive, third one is (TN) True Negative and fourth one is (TP) True positive. From this instance, TP stands for bounding boxes that contain properly identified target vegetables crops; FP for bounding boxes that contain mistakenly identified target vegetables crops; and FN for unidentified target vegetables crops for which no bounding boxes were drawn. The results metrics of analytical ability employed include recall, precision, and F1 score. Here is a definition of recall and precision as:

$$\text{Precision}=\frac{True\ Positive}{True\ Positive+False\ Positive} \quad (10)$$

$$\text{Recall}=\frac{True\ Postive}{True\ Positive+False\ Negative} \quad (11)$$

Table 3: Initialization Parameters CenterNet

Image size for input	group	Momentum	Initial Learning rate	Decay	Training steps
512X512	4	0.9	$1.25e^{-4}$	0.0001	55,200

Table 4: Analyzing Various Confidence Scores

CS	TP	FP	P	R	F1 Score
0.9	1327	12	0.991	0.84	0.909
0.8	1422	33	0.977	0.90	0.937
0.7	1469	44	0.971	0.93	0.950
0.6	1501	69	0.956	0.95	0.953
0.5	1533	111	0.932	0.97	0.951

Table 5: Genetic Algorithm Variables & Results Outcome

	Results of Performance and GA Variables	values
Parameters	Population size	200
	collection	Roulette wheel selection
	intersect probability	0.8
	change rate	0.2
	Number of Iterations	2000
Results	Assessment time	400000
	Making with optima	423
	BCE_{min}	0.113%
	Bayesian Classification Error	0.21%
	x	-19
	y	24
	z	-2
	T	862
Index colors		- 19R + 24G - 2B ≥ 862

The F1 Score is another crucial metric for assessing the model. It is a harmonic method of recall that is defined as follows.

$$F1=\frac{2\ XPrecisionXRecall}{PrecisionXRecall} \quad (12)$$

The PRC (Precision Recall Curve) is composed of recall and precision (horizantal axis) (vertical axis). It is a more impartial principle for making judgments when assessing the model's performance. Figure 7 displays the comparison outcomes of various IoU thresholding levels on the comibned test set recorded by Precision Recall Curves. In this investigation, the IoU thresholding value of 0.5 was used.1690 ground truth the test set's bounding boxes were utilised to assess the model and calculate the confidence scores' thresholding value (Table 4). Five threshold values were utilised and tested: 0.5, 0.6, 0.7, 0.8, and 0.9. The best value was determined to be 0.6, which produced a precision and recall of 95.8% and 95%, respectively.

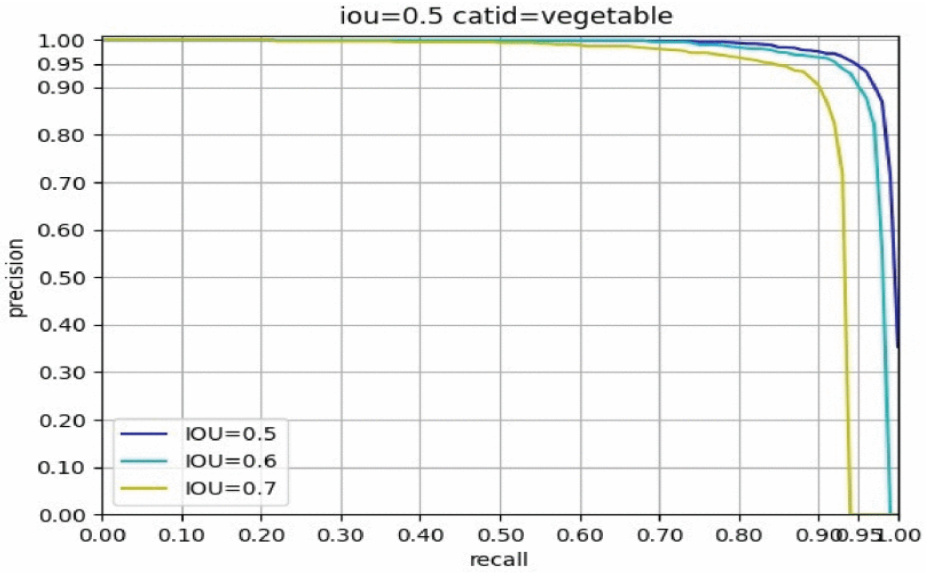

Figure 7: IoU Thresholding Curve for Precision-recall with Various Values

Fig. 8 displays how the trained model performed on pictures obtained under variety of scenarios (Figure two). The outcome pictures proved that the Center Net identification model can offer highly accurate categorization. The proposed deep learning model can therefore be used to identify the vegetable.

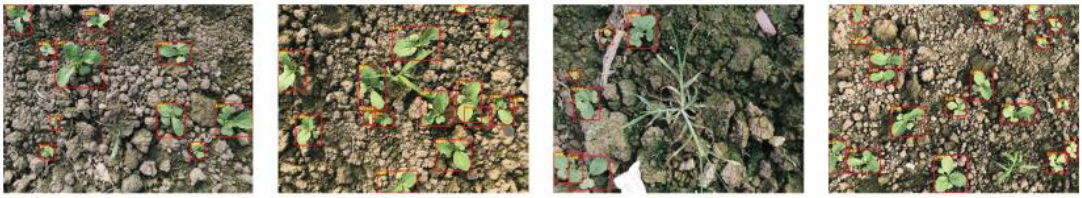

(Fig.8: a) (Fig.8: b) (Fig.8: c) (Fig.8: d)

Figure 8: Vegetable Detection using the CenterNet Detection Model in Varied Environments

Fig. 9 illustrates how to identify vegetables when broadleaf weed is present. The results indicate that the trained CenterNet specification can effectively distinguish between vegetables and broadleaf weeds. It's crucial to acknowledge the significant diversity among weed species. Traditionally, identifying weeds directly has been the standard method. To classify weeds, deep learning models need training on diverse weed datasets. Detection may fail if a particular weed type hasn't been encountered in the training dataset. In contrast, the proposed approach focuses on instructing the model to exclusively recognize vegetables, eliminating the necessity to handle various weed types. Even in the presence of unidentified weeds, the likelihood of misidentification is minimized.

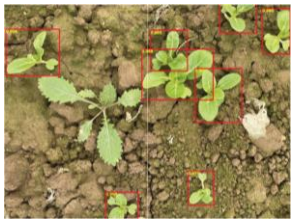

Figure 9: Finding Vegetables When Broadleaf Weed is Present

Examining the detection situations also indicated that occlusion may cause a veggie to be missed (Fig. 10). In Fig. 10, a number of veggies were planted too closely together and became totally obscured. Missing identification would be the result of running into such situations in the field. However, by including increased obscurations in the training dataset, this case can be further enhanced or resolved. Furthermore, because vegetables often have smaller canopies and do not have any reach very far at this stage of growth, better results should be obtained with a more advanced growth stage (Lammie, C., 2019).

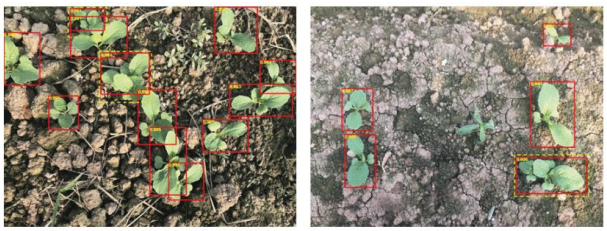

(Fig.10: a) (Fig.10: b)

Figure 10: Missed Vegetable Cases are Enclosed in the Yellow Boxes with Dashed Lines. Occlusion of (a-b)

Weed Segmentation Performance

20 photos under diverse settings were chosen as reference photographs for the GA trials. The identical selection of four unsegmented photos from Fig. 8 were also utilised as test images to assess the performance of the GA colour index segmentation algorithm. According to Eq. 9, the reference pictures' BCEmin theoretical minimum value was 0.113%. Table 5 displays the GA settings and performance outcomes.

The best fitness value using any population under 2126 generations, regardless of size, BCE function was 0.21%. When the population size or iterations were increased, best fitness did not significantly improve. The colour index's associated outcome is as follows:

$$\begin{cases} -19R + 24G - 2B \geq 862, & weed \\ -19R + 24G - 2B < 862, & Background \end{cases} \quad (13)$$

Outputs of the applying index of the proposed algorithm to the images in Figure 8 are shown in Figure 11, which demonstrate that weeds are successfully separated from circumstances for pictures shot in the wild. Evaluation was done by contrasting the segmentation result with the excess green index (ExG) index in order to further confirm segmentation results.

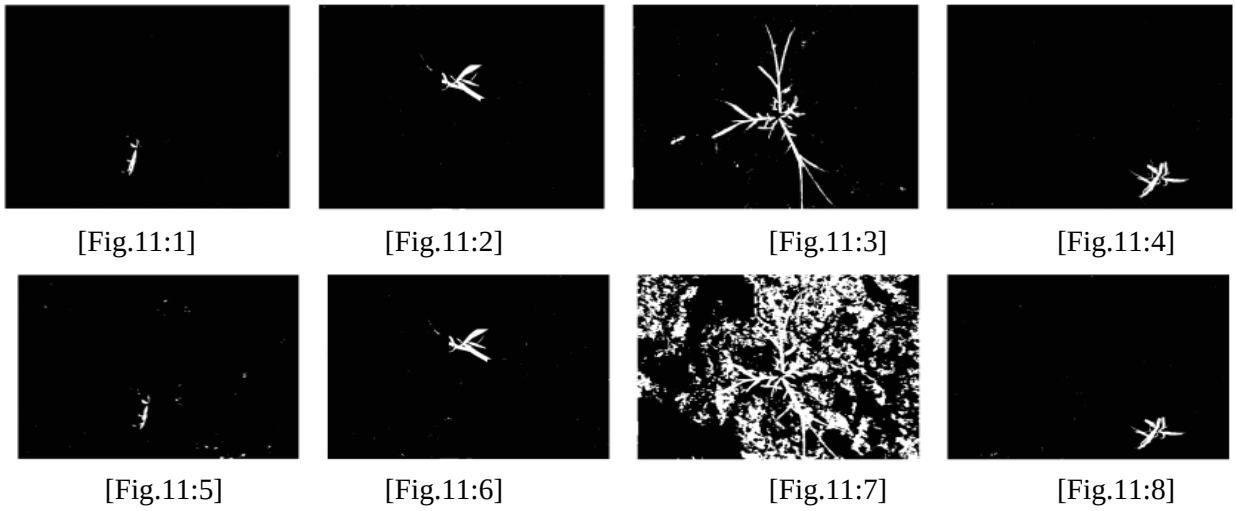

[Fig.11:1] [Fig.11:2] [Fig.11:3] [Fig.11:4]

[Fig.11:5] [Fig.11:6] [Fig.11:7] [Fig.11:8]

Figure 11: Application of the Excess Green Index + Otsu to the Photos in Fig. 8(a) Yielded Desired Results

The ExG index is frequently used and has shown to be effective at distinguishing crops from circumstances (Hamuda, E., 2016). Excess Green index translated colour images into gray scale images, which are easily converted into black-and-white images using the Otsu method to extract binary images. Examining Fig. 11 revealed that the ExG + Otsu method's result was tainted by additional noises and unable to distinguish weeds from a complicated background (Fig. 11:6). ExG + Otsu method's performance in this study is worse than the suggested colour index because ExG + Otsu threshold frequently leads to under-segmentation. ExG segmentation, on the other hand, takes more time to compute because it involves two phases.

Table 6 illustrates the BCEs and processing times for the PI and Excess Green Index + Otsu in comparison. According to the BCEA metric, it is clear that the suggested index produces high segmentation quality at a significantly less computing cost than Excess Green Index + Otsu technique,

making it acceptable for use in crops and vegetable plantations under natural circumstances for smart mechanical weed management.

Table 6: Comparisons Among ExG + Otsu and the Planned Index

Test Image	Bayesian Classification Error		Running Timing(milisec.)	
	PI	ExG + Otsu	PI	ExG + Otsu
Figure 8(a)	0.032%	0.097%	5.326	9.35
Figure 8(b)	0.009%	0.019%	5.24	8.43
Figure 8(c)	0.189%	12.40%	6.89	10.2
Figure 8(d)	0.024%	0.025%	6.09	8.87

were PI denoting Proposed Index.

In order to create a colour index that might work in multiple lighting conditions, a number of images were taken in various lighting conditions were selected as reference images throughout the GA searching. When the suggested index was used to analyze the low- and high-brightness photographs in Figure 8a and 8b, respectively. The segmentation results are shown in Figs. 11:1 and Figs.11:2. This demonstrates that weeds were successfully segmented from background for images taken under various lighting conditions. Some backdrop pixels were mistakenly identified as weeds because of the colour resemblances between them and the background (noises). These noises were typically dispersed randomly over the image. The relatively small noise patches in the binary image were removed using an area filter and a thresholding approach. Each related region's area was determined. Smaller objects were regarded as noise and filtered using a predetermined threshold that was developed through trial and error (Fig. 12a, Fig. 12b, Fig. 12c, Fig. 12d). The final segmentation findings are displayed in Figures 13a, 13b, 13c, and 13d with the vegetable regions denoted by red boxes. The segmentation of different vegetation in agricultural areas using the proposed GA approach using the Bayesian classification error Algorithm fitness function can also be done by calculating colour indices. By simply swapping out the reference photos and tallying the pixel distribution probabilities of the matching targets, this technique may also be easily duplicated.

(Fig.12: a) (Fig.12: b) (Fig.12:c) (Fig.12: d)

Figure 12: Results After Applying Area Filter (a) on fig. 11(a), 11(b), 11(c), and 11 (d)

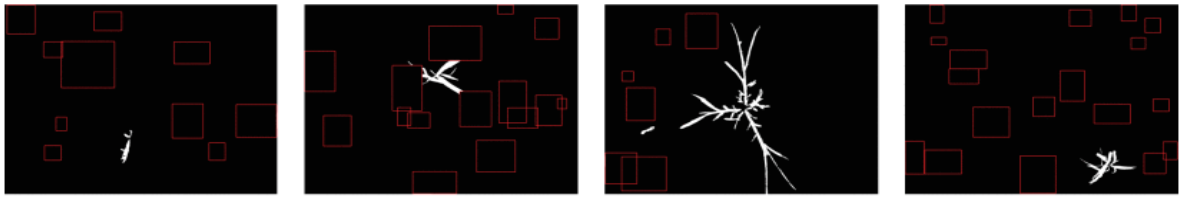

(Fig.13: a) (Fig.13: b) (Fig.13:c) (Fig.13: d)

Figure 13: Vegetable Regions that Make up the Last Segment are Highlighted in Red

4 Conclusion

In this paper used forth a method for employing deep learning and image processing to find weeds in vegetable plantations. Two steps made up the algorithm's representation. Vegetable detection was taught to a CenterNet model. The trained CenterNet attained a Figure1 score of 0.953, a precision of 95.6%, and a recall of 95.0%. The remaining green items that were present in the colour image were then regarded as weeds. A color index was established and evaluated utilizing Genetic Algorithms (GAs) based on Bayesian classification error to distinguish weeds from the background. This method, by focusing solely on the detection of vegetables, allows the model to sidestep the complexities associated with various weed species.

This research article made the following contributions: 1) Deep learning and image processing research and presentation of a technique for weed identification in vegetable plantations 2) Develop a brand-new, deceptive optical trick to tell weeds from vegetables. 3) Propose a colour scale to help people in real-world situations tell weeds apart from the background. Despite only being relevant to organic vegetables, the anticipated algorithm in this research study can be used for smart mechanical or chemical robotic weeding. The research's excellent findings confirmed that the suggested methodology is more suitable for beginning and ground-based weed detection and identification in growing crops and vegetable plantations below a range of circumstances, including complex backgrounds, varying illumination, as well as several stages of growth, and has application value for the growth of the vegetable industry sustainably.

References

[1] Bae, D., & Ha, J. (2021). Performance Metric for Differential Deep Learning Analysis. *Journal of Internet Services and Information Security (JISIS), 11*(2), 22-33.

[2] Benos, L., Tagarakis, A.C., Dolias, G., Berruto, R., Kateris, D., & Bochtis, D. (2021). Machine learning in agriculture: A comprehensive updated review. *Sensors*, *21*(11), 1-55.

[3] Berge, T.W., Aastveit, A.H., & Fykse, H. (2008). Evaluation of an algorithm for automatic detection of broad-leaved weeds in spring cereals. *Precision Agriculture*, *9*, 391-405.

[4] Bermant, P.C., Bronstein, M.M., Wood, R.J., Gero, S., & Gruber, D.F. (2019). Deep machine learning techniques for the detection and classification of sperm whale bioacoustics. *Scientific reports*, *9*(1), 1-10.

[5] Dai, X., Xu, Y., Chen, J., & Zheng, J. (2020). Evaluation of mixing uniformity for inline mixers by image processing. *Transactions of the ASABE*, *63*(2), 429-443.

[6] Dai, X., Xu, Y., Zheng, J., & Song, H. (2019). Analysis of the variability of pesticide concentration downstream of inline mixers for direct nozzle injection systems. *Biosystems Engineering*, *180*, 59-69.

[7] Dai, X., Xu, Y., Zheng, J., Ma, L., & Song, H. (2020). Comparison of image-based methods for determining the inline mixing uniformity of pesticides in direct nozzle injection systems. *Biosystems Engineering*, *190*, 157-175.

[8] Gu, H., & Choo, S. (2022). Method for Constructing a Façade Dataset through Deep Learning-Based Automatic Image Labeling. *Applied Sciences*, *12*(15), 1-17.

[9] Gutiérrez, S., Hernández, I., Ceballos, S., Barrio, I., Díez-Navajas, A.M., & Tardaguila, J. (2021). Deep learning for the differentiation of downy mildew and spider mite in grapevine under field conditions. *Computers and Electronics in Agriculture*, *182*.

[10] Hamuda, E., Glavin, M., & Jones, E. (2016). A survey of image processing techniques for plant extraction and segmentation in the field. *Computers and electronics in agriculture*, *125*, 184-199.

[11] Lammie, C., Olsen, A., Carrick, T., & Azghadi, M.R. (2019). Low-Power and High-Speed Deep FPGA Inference Engines for Weed Classification at the Edge. *IEEE Access*, *7*, 51171-51184.
[12] Liakos, K.G., Busato, P., Moshou, D., Pearson, S., & Bochtis, D. (2018). Machine learning in agriculture: A review. *Sensors*, *18*(8), 1-29.
[13] Nampei, M., Horikawa, M., Ishizu, K., Yamazaki, F., Yamada, H., Kahyo, T., & Setou, M. (2019). Unsupervised machine learning using an imaging mass spectrometry dataset automatically reassembles grey and white matter. *Scientific reports*, *9*(1), 1-11.
[14] Olsen, A., Konovalov, D.A., Philippa, B., Ridd, P., Wood, J.C., Johns, J., & White, R.D. (2019). Deep Weeds: A multiclass weed species image dataset for deep learning. *Scientific reports*, *9*(1), 1-12.
[15] Pawłowski, J., Majchrowska, S., & Golan, T. (2022). Generation of microbial colonies dataset with deep learning style transfer. *Scientific Reports*, *12*(1), 1-12.
[16] Rączkowski, Ł., Możejko, M., Zambonelli, J., & Szczurek, E. (2019). ARA: accurate, reliable and active histopathological image classification framework with Bayesian deep learning. *Scientific reports*, *9*(1), 1-12.
[17] Sahlsten, J., Jaskari, J., Kivinen, J., Turunen, L., Jaanio, E., Hietala, K., & Kaski, K. (2019). Deep learning fundus image analysis for diabetic retinopathy and macular edema grading. *Scientific reports*, *9*(1), 1-11.
[18] Serpen, G., & Aghaei, E. (2018). Host-based misuse intrusion detection using PCA feature extraction and kNN classification algorithms. *Intelligent Data Analysis*, *22*(5), 1101-1114.
[19] Veeranampalayam Sivakumar, A.N., Li, J., Scott, S., Psota, E., J Jhala, A., Luck, J.D., & Shi, Y. (2020). Comparison of object detection and patch-based classification deep learning models on mid-to late-season weed detection in UAV imagery. *Remote Sensing*, *12*(13), 1-22.
[20] Yu, S.H., Yun, Y.T., Choi, Y., Dafsari, R.A., & Lee, J. (2021). Effect of injection angle on drift potential reduction in pesticide injection nozzle spray applied in domestic Agricultural Drones. *Journal of Biosystems Engineering*, *46*(2), 129-138.
[21] Yu, X., Pang, W., Xu, Q., & Liang, M. (2020). Mammographic image classification with deep fusion learning. *Scientific Reports*, *10*(1), 1-11.

Authors Biography

Veerasamy, K. He received his Master degree in Computer Science from Bharathiyar University, Tamil Nadu, India in 2006, He is received his Master Degree in Computer Science Engineering from Karpagam University, Tamil Nadu, India in 2014, also worked as Assistant Professor at Bannari Amman Institute of Technology, Sathyamangalam, Erode, Tamil Nadu, he is currently working as an Assistant Professor in Department of Computer Science in Karpagam Academy of Higher Education, Coimbatore, Tamil Nadu and also he is currently pursuing his Ph.D in Computer Science in Karpagam Academy of Higher Education, Coimbatore, Tamil Nadu, India. He presented more than 10 papers in International Conferences. He has published many papers in the reputed International and National Journals.

Thomson Fredrik, E.J. He received his MCA degree from Bharathiar University, Coimbatore. He did his Ph. D Degree in Computer Science from Bharthiar University, Coimbatore. He is currently working as a Professor in the Department of Computer Technology at Karpagam Academy of Higher Education, Coimbatore. He has 20 years of teaching experience. He has produced Six Ph. D Scholars in Computer Science under his guidance. He has published one patent in Internet of Things and two patents in Artificial Intelligence. He presented more than 10 papers in International Conferences. He has published many papers in the reputed International and National Journals. He has published two books and four book chapters in the Springer Lecture Series. His research interests include Artificial Intelligence and Data Mining.